TEXTURE ANALYSIS OF LESION PERFUSION VOLUMES IN DYNAMIC CONTRAST-ENHANCED BREAST MRI

Sang Ho Lee[1,3], Jong Hyo Kim[1,2,3], Jeong Seon Park[2], Jung Min Chang[2], Sang Joon Park[1,3], Yun Sub Jung[1,3], Sungho Tak[4], Woo Kyung Moon[2]

[1]Interdisciplinary Program in Radiation Applied Life Science major, [2]Department of Radiology, [3]Institute of Radiation Medicine, Seoul National University College of Medicine, Seoul, Korea; [4]Department of Bio and Brain Engineering, Korea Advanced Institute of Science and Technology (KAIST), Daejeon, Korea

ABSTRACT

This study introduces a novel texture analysis scheme applied to perfusion volumes in dynamic contrast-enhanced (DCE) breast MRI to provide a method of lesion discrimination. DCE MRI was applied to 24 lesions (12 malignant, 12 benign). Automatic segmentation was performed for extraction of a lesion volume, which was divided into whole, rim and core volume partitions. Lesion perfusion volumes were classified using three-time-points (3TP) method of computer-aided diagnosis. Receiver operating characteristic curve (ROC) analysis was performed for differentiation of benign and malignant lesions using texture features of perfusion volumes classified by the 3TP method. When using the texture features of perfusion volumes divided into rim and core lesion volume, the texture features to have more improved accuracy appeared than using whole lesion volume. This result suggests that lesion classification using texture features of local perfusion volumes is helpful in selecting meaningful texture features for differentiation of benign and malignant lesions.

Index Terms— Texture analysis, breast MRI, co-occurrence matrices, 3TP method, tumor segmentation

1. INTRODUCTION

Dynamic contrast-enhanced (DCE) MR imaging is now an integral part of a proposed standard diagnostic protocol for breast cancer [1]. The advantages of this approach originate from the observation that the quantitative time courses of MR imaging signal intensity appear to be capable of enabling differentiation of benign and malignant lesion [2]. Thus, signal-intensity time course after injection of contrast agent was determined to evaluate the perfusion characteristics of enhancing breast lesions.

Several studies have reported a marked difference between the slope of enhancement uptake of benign and malignant lesions: malignant lesions enhance earlier and greater than benign lesions [3], [4]. Kuhl et al. have showed that use of curve shape (washout, plateau, or persistent enhancement) based on three-time-points (3TP) method, which generates a colormap allowing pixel-by-pixel kinetic analysis from the intensity values measured at three judiciously chosen time points: the pre-contrast time plus two post-contrast times, can distinguish malignant lesions from benign and demonstrated that this approach is more reliable in comparison with the slope of enhancement uptake [5], [6].

Evaluating the information of DCE-MRI is a demanding task for the human observer due to the multivariate nature of the data, so the diagnosis is time consuming and frequently suffers from inter-and intra-observer variability [7]. The placement of regions of interest (ROIs) for measuring averaged temporal kinetic signals or the evaluation of morphological features is subjective and strongly depends on the observer's experience. Collins and Padhani have indicated that whole tumor ROIs is inappropriate for evaluation of malignant lesions and analysis of imaging data needs to reflect the heterogeneity of tumor vascular characteristics [8]. The heterogeneity of tumor vasculatures can be quantified by texture analysis of computer-aided diagnosis (CAD).

The work presented in this study uses three-dimensional (3D) co-occurrence-based texture analysis of a novel approach to distinguish between benign and malignant lesions from DCE-MR images. With the use of texture analysis, statistical information regarding lesion voxels, which reflect the class label assigned by 3TP method after automatic segmentation of a lesion, is gathered. In addition, this analysis is performed based on the hypothesis which texture features of local perfusion volumes such as tumor rim and/or core are more helpful for differentiation of benign and malignant lesions. The purpose of this study is to classify of 3D texture features of perfusion volumes assigned by 3TP method and to examine meaningful texture features

having improved accuracy in discrimination between benign and malignant lesions.

2. MATERIALS AND METHODS

2.1. Materials and Protocols

DCE-MRI was applied to 24 lesions (12 malignant, 12 benign) using 1.5 T Sonata (Siemens, Erlangen, Germany). First, the pre-contrast T1 weighted 3D fast low angle shot (FLASH) sagittal image (TR 4.9 ms, TE 1.83 ms, FA 12°, FOV 170 mm, matrix 448×448, acquisition time 84 s, slice thickness 1-1.4 mm without gap) was obtained with fat suppression and next four consecutive post-contrast images using the same condition after an injection of 0.1 mmol/kg Gd-DTPA (Magnevist, Schering, Berlin, Germany). The contrast material was administered manually at a flow rate of 2 ml/s for 5 sec and imaging was performed within 15 sec after injecting the contrast agent.

2.2. Thresholding of Suspicious Regions

3D rigid registration (fixed image, pre-contrast image; moving image, post-contrast images) were performed for reducing the artifacts of patient movement, where tissue deformation was not considered in order to avoid excessive modification of original grey levels. Initially, we constructed our proposed perfusion index (PI) using both signal intensity and enhancement curves for subsequently extracting suspicious regions by the threshold as the following expression.

$$PI = \frac{MI}{k} + \sum_{i=1}^{N} PE_i \cdot (Post_i - Pre) + \sum_{i=1}^{N-1} SER_i \cdot (Post_i - Post_N) \quad (1)$$

where $PE_i = \frac{Post_i - Pre}{Pre}$ and $SER_i = \frac{Post_i - Pre}{Post_N - Pre}$

Thresholding of suspicious regions was based on the nonparametric and unsupervised method of automatic threshold selection presented by Otsu [9].

Table 1. Notations used in the expression (1)

MI	The maximum intensity value among all post-contrast series
k	The series number of the maximum intensity phase
PE_i	Percent enhancement of the *i*th series
SER_i	Signal enhancement ratio of the *i*th series
$Post_i$	The *i*th post-contrast image
$Post_N$	The last post-contrast image
Pre	Pre-contrast image
N	The total number of post-contrast series

2.3. Lesion Segmentation

The connected threshold region growing segmentation was performed in order to extract a connected component from a user-defined seed on the threshold image, and hole-filling on its segmented region. Sphericity and center distance of mass to surface area ratio on the threshold image were used for determining whether the segmented volume should be eroded or not, and the number of erosion if the segmented volume should be erode. While erosion was performed repeatedly on the segmented volume, the connected threshold region growing segmentation followed each erosion. Dilation was initially executed by the equal number of erosion operation and next performed in the range above the median value between maximum and mean values of PI within dilation volume in order to compensate speculate lesion boundary removed by erosion. Finally, erosion of whole lesion volume was performed until the volume after erosion operation was under 1/3 of whole lesion volume for separating the lesion rim and core volumes.

2.4. 3TP Classification

The enhancement curves for each lesion were classified based on the criteria of the 3TP method. The enhancement properties were quantified by computing the PE_1 and SER_1 (Figure 1).

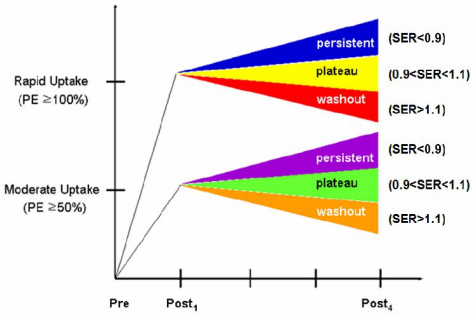

Figure 1. Voxel classification scheme based on PE and SER values

2.5. Texture Analysis

A second-order joint conditional histogram (also called a co-occurrence matrix) is computed given a specific distance between pixels and a specific direction. The two random variables are the class label of one pixel (c_1) and the class label of its neighboring pixel (c_2), and the neighborhood between two pixels is defined by a user-specified distance and direction. Once a co-occurrence matrix is computed, statistical parameters can be calculated from the matrix.

For an N_c class label image, I, the co-occurrence matrix is defined as:

$$P_{\theta,d}(i,j) = \sum_{l=1}^{L}\sum_{m=1}^{M}\sum_{n=1}^{N} \rho(I(l,m,n), I(l',m',n'), i, j) \quad (2)$$

where the image size is $L \times M \times N$, d and θ are distance and direction between pixel pair $<I(m, n), I(m', n')>$ and ρ is defined as:

$$\rho(I(l,m,n), I(l',m',n'), i, j) = \begin{cases} 1 & \text{if } I(l,m,n) = i \text{ and } I(l',m',n') = j \\ 0 & \end{cases}$$

The elements of co-occurrence matrix, $p_{\theta,d}(i, j)$, represent the relative frequency by which two pixels with class labels i and j, that are at a distance d in a given direction θ, are in neighborhood. The immediate neighbors of any pixel (d=1) can lie on thirteen possible directions, $\theta=(\theta_1, \theta_2)$=(0°, 0°), (0°, 45°), (0°, 90°), (0°, 135°), (45°, 0°), (45°, 45°), (45°, 90°), (45°, 135°), (90°, NA), (135°, 0°), (135°, 45°), (135°, 90°) and (135°, 135°). Texture calculations are best performed on symmetrical matrices. It is seen that:

$$P(d, -\theta) = P^T(d, \theta) \tag{3}$$

where $P^T(d, \theta)$ is the transpose of $P(d, \theta)$. Thus, a symmetric co-occurrence matrix is given by:

$$P_s(d, \theta) = \frac{1}{2}\left[P(d, \theta) + P^T(d, \theta)\right] \tag{4}$$

Assuming isotropy (no direction) we can pool the frequencies of co-occurrence matrices with different orientations θ and approximately the same distance d. This provides a directional invariant co-occurrence matrix.

$$\begin{aligned} P_{isotropic}(d) = \frac{1}{13}[&P_s(d, (0^\circ, 0^\circ)) + P_s(d, (0^\circ, 45^\circ)) \\ &+ P_s(d, (0^\circ, 90^\circ)) + P_s(d, (0^\circ, 135^\circ)) \\ &+ P_s(d, (45^\circ, 0^\circ)) + P_s(d, (45^\circ, 45^\circ)) \\ &+ P_s(d, (45^\circ, 90^\circ)) + P_s(d, (45^\circ, 135^\circ)) \\ &+ P_s(d, (90^\circ, \mathrm{NA})) \\ &+ P_s(d, (135^\circ, 0^\circ)) + P_s(d, (135^\circ, 45^\circ)) \\ &+ P_s(d, (135^\circ, 90^\circ)) + P_s(d, (135^\circ, 135^\circ))] \end{aligned} \tag{5}$$

The elements $C(i, j)$ of normalized direction invariant co-occurrence matrix C is given by:

$$C(i, j) = \frac{P_{isotropic}(i, j)}{\sum_{i,j=1}^{Nc} P_{isotropic}(i, j)} \tag{6}$$

Where $P_{isotropic}(i, j)$ are the elements of the isotropic co-occurrence matrix and N_c is the number of classes assigned by the 3TP method. In this study, we used a distance value of one to generate the co-occurrence matrices, and eight texture features: contrast (CON), correlation (COR), dissimilarity (DIS), entropy (ENT), inverse difference moment (IDM), inverse difference (INV), uniformity (UNI) and maximum probability (MAX) (Table 2).

Table 2. Co-occurrence matrix derived texture features

Feature No.	Feature Name	Formula
1	CON	$\sum_{i,j}(i-j)^2 C(i,j)$
2	COR	$\sum_{i,j}\frac{(i-\mu_x)(j-\mu_y)}{\sigma_x\sigma_y}$ where $\mu_x=\sum_i i\sum_j C(i,j)$, $\mu_y=\sum_j j\sum_i C(i,j)$, $\sigma_x=\sum_i(i-\mu_x)^2\sum_j C(i,j)$, $\sigma_y=\sum_j(j-\mu_y)^2\sum_i C(i,j)$
3	DIS	$\sum_{i,j}(\lvert i-j\rvert^k)^2 C(i,j)$ where $k=1$ and $i \neq j$
4	ENT	$-\sum_{i,j} C(i,j)\log C(i,j)$
5	IDM	$\sum_{i,j}\frac{C(i,j)}{1+(i-j)^2}$
6	INV	$\sum_{i,j}\frac{C(i,j)}{1+\lvert i-j\rvert}$
7	UNI	$\sum_{i,j} C(i,j)^2$
8	MAX	$\max C$

3. RESULTS

The 3TP classification results were shown within a lesion volume by different colors reflecting each enhancement pattern. Homogeneity or heterogeneity of the enhancement patterns within the lesion volume was able to be visually identified and the eight texture features confirmed (Figure 2). Table 3 shows the results of ROC analyses using texture features in whole, rim and core lesion volumes, respectively. With the use of texture features which were calculated by separating rim and core volumes of a lesion, more improved sensitivity or specificity was seen than using whole lesion volume. The texture features within core lesion volume showed higher sensitivity in COR, IDM and INV than others, and the texture features within rim lesion volume relatively higher specificity in CON, COR, ENT, IDM, INV, UNI and MAX and relatively higher accuracy in all features.

Table 3. The results of ROC analyses

Lesion volume	Feature	Sensitivity	Specificity	Accuracy
Whole	CON	83.3 %	58.3 %	71.5 %
	COR	83.3 %	50 %	67.4 %
	DIS	83.3 %	66.7 %	72.9 %
	ENT	100 %	41.7 %	68.1 %
	IDM	75 %	75 %	74.3 %
	INV	75 %	75 %	74.3 %
	UNI	100 %	41.7 %	68.1 %
	MAX	100 %	41.7 %	65.3 %
Rim	CON	83.3 %	66.7 %	79.9 %
	COR	66.7 %	75 %	69.4 %
	DIS	83.3 %	66.7 %	78.5 %
	ENT	83.3 %	66.7 %	77.8 %
	IDM	75 %	83.3 %	79.9 %
	INV	75 %	83.3 %	79.9 %
	UNI	83.3 %	66.7 %	75.7 %
	MAX	83.3 %	66.7 %	70.1 %
Core	CON	83.3 %	58.3 %	58.3 %
	COR	100 %	41.7 %	56.9 %
	DIS	83.3 %	58.3 %	63.2 %
	ENT	100 %	41.7 %	64.6 %
	IDM	83.3 %	58.3 %	64.6 %
	INV	83.3 %	58.3 %	66.7 %
	UNI	100 %	41.7 %	63.2 %
	MAX	100 %	41.7 %	62.5 %

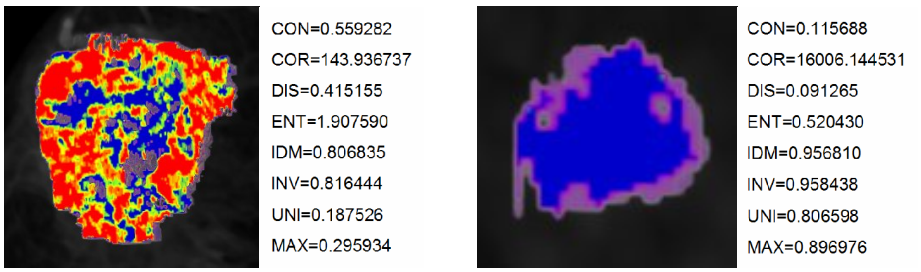

(a) (b)

Figure 2. Examples of color maps of enhancement patterns assigned by the 3TP method and texture features within whole volume of (a) malignant and (b) benign lesions

5. DISCUSSION

This study provides new insight which computationally verifies texture features combined with the 3TP method familiar with radiologists within a lesion. In addition, this study considers the importance of lesion segmentation before the 3TP classification and texture analysis. The appropriate selection of initial lesion segmentation method is important for obtaining accurate characteristics of texture features within a lesion because the inclusion of normal tissue components outside a lesion is able to disturb the discrimination between benign and malignant lesions using texture features. Thus, we constructed that the difference of kinetic features between a lesion and normal tissue components was maximized by PI, and were able to achieve effective thresholding of suspicious regions by Otsu threshold method, which finds an optimal threshold that separates the two main classes of an image, background and foreground.

Previous studies have reported the results from using texture features in breast DCE-MRI. Tzacheva et al. only used region-based analysis rather than voxel-by-voxel analysis and does not take advantage of the voxel signal intensity changes over the entire DCE-MRI time sequence [10]. Lucht et al. did not show a good sensitivity (84%) or specificity (81%) for discrimination between benign and malignant lesion voxels [11]. On the other hand, this study uses texture features of curve types assigned by the 3TP method on a voxel-by-voxel basis and shows possibility to surpass existing results. In addition, this study suggests that use of texture features which are separated by rim and core lesion volumes was advantageous to diagnostic accuracy, considering the characteristic which malignant lesions have relatively more distinct rim enhancement and more heterogeneous textures. In the future, it is necessary to demonstrate the usefulness of the texture features combined with the 3TP method after collecting more patient data.

5. CONCLUSION

This result indicates that lesion classification using texture features of local perfusion volumes within a lesion is helpful in selecting texture features for differentiation of benign and malignant lesions.

11. REFERENCES

[1] S.E. Harms, "Technical report of the international working group on breast MRI", *J Magn Reson Imaging*, vol. 10, pp. 979-1015, 1999.

[2] M.V. Knopp, E. Weiss, H. P. Sinn, J. Mattern, H. Junkermann, J. Radeleff, A. Magener, G. Brix, S. Delorme, I. Zuna, and G. van Kaick, "Pathophysiologic Basis of Contrast Enhancement in Breast Tumors", *J Magn Reson Imaging*, vol. 10, pp. 260-266, 1999.

[3] S.H. Heywang-Kobrunner, "Contrast-enhanced magnetic resonance imaging of the breast", *Invest Radiol*, vol. 29, pp. 94-104, 1994.

[4] W.A. Kaiser, and E. Zeitler, "MR imaging of the breast: fast imaging sequences with and without Gd-DTPA. Preliminary observations", *Radiology*, vol. 170, pp. 681-686, 1989.

[5] C.K. Kuhl, P. Mielcareck, S. Klaschik, C. Leutner, E. Wardelmann, J. Gieseke, and H. H. Schild, "Dynamic Breast Imaging: Are Signal Intensity Time Course Data Useful for Differential Diagnosis of Enhancing Lesions?", *Radiology*, vol. 211, pp. 101-110, 1999.

[6] H. Degani, V. Gusis, D. Weinstein, S. Fields, and S. Strano, "Mapping pathophysiological features of breast tumors by MRI at high spatial resolution", *Nature Medicine*, vol. 3, pp. 780-782, 1997.

[7] S.G. Orel, and M.D. Schnall, "MR imaging of the breast for the detection, diagnosis, and staging of breast cancer", *Radiology*, vol. 220, pp. 13-30, 2001.

[8] D.J. Collins, and A.R. Padhani, "Dynamic magnetic resonance imaging of tumor perfusion", *IEEE Eng Med Biol Mag*, vol. 23, pp. 65-83, 2004.

[9] N. Otsu, "A threshold selection method from gray-level histograms", *IEEE Transactions on Systems, Man, and Cybernetics*, vol. SMC-9, pp. 62-66, 1997.

[10] A.A. Tzacheva, K. Najarian, J. Brockway, "Breast cancer detection in gadolinium-enhanced MR images by static region descriptors and neural networks", *J Magn Reson Imaging*, vol. 17, pp. 337-342, 2003.

[11] R. Lucht. M. Knopp, G. Brix, "Classification of signal-time curves from dynamic MR mammography by Neural Networks", *Magn Reson Imaging*, vol. 19, pp. 51-57, 2001.